

Monte Carlo simulation of the measurement by the 2E technique of the average prompt neutron multiplicity as a function of the mass of fragments from thermal neutron-induced fission of ^{239}Pu

M. Montoya*, O. Páucar, A. Obregón, and A. Aponte

Universidad Nacional de Ingeniería,
Av. Túpac Amaru 210, Rímac, Lima, Perú
*e-mail: mmontoya@uni.edu.pe

Received 7 July 2021; accepted 30 August 2021

Using a Monte Carlo method, we simulate the measurement, by the 2E technique, of the average prompt neutron multiplicity as a function of the mass of fragments from the thermal neutron induced fission of ^{239}Pu . The input data for the simulation, associated with the primary fragment mass (A), consist of the yield (Y), the distribution of the total kinetic energy characterized by its average (\overline{TKE}) and its standard deviation (σ_{TKE}), the average prompt neutron multiplicity ($\bar{\nu}_s$, a sawtooth approach of experimental data), and the slope of neutron multiplicity against total kinetic energy ($d\nu_s/d < TKE >$). The output data, associated with the simulated as the fragment mass measured by the 2E technique (μ), consist of the yield (y), the distribution of the total kinetic energy characterized by its average (\overline{tke}) and its standard deviation (σ_{tke}), and the average prompt neutron multiplicity ($\bar{\nu}_\mu$). In the mass regions $A \approx 115$ and $A > 150$, $\bar{\nu}_\mu$ is higher than $\bar{\nu}_s$. This result suggests that, in those mass regions, the 2E experimental values associated with the average neutron multiplicity are overestimated, referred to the corresponding to the primary fragments.

Keywords: Nuclear fission; fission product yield; prompt neutron multiplicity; fission fragment kinetic energy; plutonium 239.

DOI: <https://doi.org/10.31349/RevMexFis.68.011201>

1. Introduction

The nuclear fission of actinides begins at the saddle point of the fission barrier when the fissile nucleus is deformed without return and ends at the scission point, from which the fragments separate acquiring their final kinetic energy by Coulomb repulsion. Before and after the scission point neutrons are emitted [1].

One of the quantities proper to study fission dynamics is the average prompt neutron multiplicity as a function of the primary mass of fragments ($\bar{\nu}$). However, because prompt neutron emission, it is not possible to measure the primary fragment mass; and the experimental values associated with $\bar{\nu}$ as a function of fragment mass depend on the used measurement technique. This has been shown for reactions $^{233}\text{U}(\text{nth}, \text{f})$, $^{235}\text{U}(\text{nth}, \text{f})$, $^{252}\text{Cf}(\text{sf})$ [2-10], $^{239}\text{Pu}(\text{nth}, \text{f})$ [11-15], and spontaneous fission of ^{252}Cf [16], respectively.

Recently, a Monte Carlo simulation of the measurement by the 1V1E technique has been performed and applied to the case of $^{239}\text{Pu}(\text{nth}, \text{f})$ [17]. In this work, a simulation of the measurement by the 2E technique is performed and applied to that reaction.

The 2E technique consists of calculating the mass of the complementary fission fragments using the measured values of kinetic energy in the momentum conservation relations. Furthermore, conservation of the number of nucleons in the reaction is assumed.

The uncertainty of the value of the kinetic energy is proportional to the number of neutrons emitted before the fragment reaches the detector. The average number of neutrons depends on the mass of the fragment. Added to this is the

resolution of the energy measurement, which depends on the detector. As an example, the total resolution of the mass of the Göök *et al.* experiment is 4 u [18].

2. Input data of the simulation

In the simulation of neutron emission, the state of deformation of the fragments is not considered. Furthermore, the

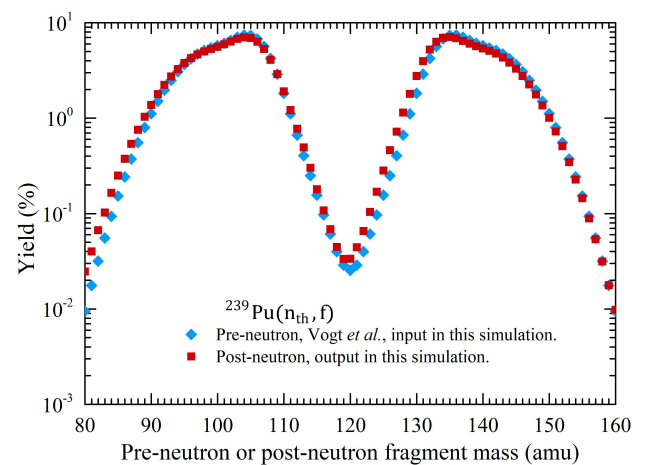


FIGURE 1. Simulation of the measurement by the 2E technique of the mass yield of fragments from the $^{239}\text{Pu}(\text{nth}, \text{f})$ reaction. We show the yield of the primary fragment mass ($Y(A)$ diamonds, taken from Ref. [19].) and the yield of simulated as measured (by 2E technique) fragment mass ($y(\mu)$, squares), which are the input and output data, respectively, in the simulation.

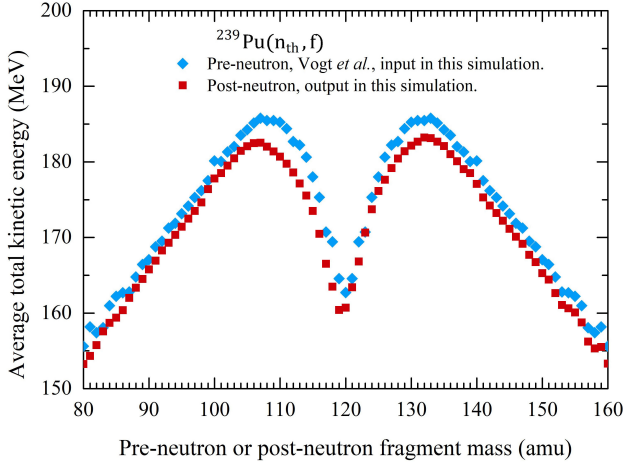


FIGURE 2. Simulation of the measurement by the 2E technique of the average total kinetic energy as a function of the mass of fragments from the $^{239}\text{Pu}(\text{nth}, \text{f})$ reaction. We show the average total kinetic energy as a function of the primary fragment mass (diamonds, values taken from Ref. [19]) and the corresponding to the pseudo mass (squares), which are the input and output data, respectively, in the simulation.

symmetry or asymmetry characteristics of the kinetic energy distribution of the fragments are not distinguished.

The input data are quantities associated with the primary complementary fragments, *i.e.*, the mass numbers (A and A' , respectively), the kinetic energy (E and E' , respectively) and the number of neutrons emitted by each fragment (n and n' , respectively).

As a function of one of the primary complementary fragments mass (A), we use the following quantities: the yield Y (Data taken from Ref. [19]. See Fig. 1); a Gaussian distribution of total kinetic energy of complementary fragments

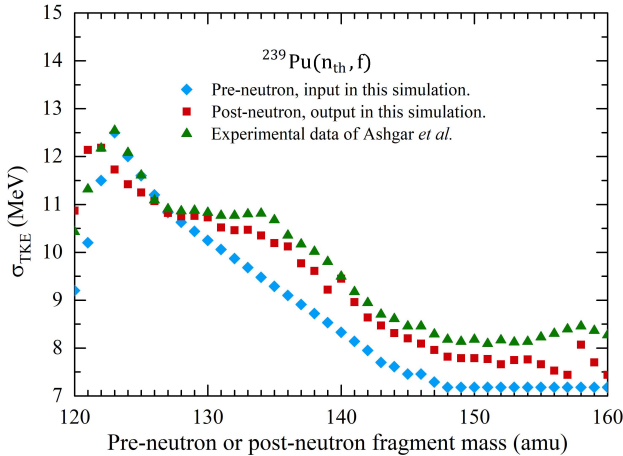


FIGURE 3. Simulation of the measurement by the 2E technique of standard deviation of the total kinetic energy distribution as a function of the mass of fragments from the $^{239}\text{Pu}(\text{nth}, \text{f})$ reaction. We show the standard deviation of the total kinetic energy distribution as a function of the primary fragment mass (diamonds) and the corresponding to the pseudo mass (squares), which are the input and output data, respectively, in the simulation. For comparison, experimental values (triangles, from Ref. [20]) are presented.

($TKE = E + E'$) with its average \overline{TKE} (Data taken from Ref. [19]. See Fig. 2), and its standard deviation σ_{TKE} (An approximation of the experimental curve taken from Ref. [20]. See Fig. 3); the average prompt neutron multiplicity $\bar{\nu}_s$ (A sawtooth approach of data taken from Ref. [13]. See Fig. 4); and the slope of the neutron multiplicity against total kinetic energy, $d\nu/d \langle TKE \rangle$ (An approach to experimental data taken from Ref. [13], See Fig. 5). The prompt neutron multiplicity as a function of total kinetic energy is assumed to be

$$\nu_s(A, TKE) = \bar{\nu}_s(A) \times \left(1 - \frac{d\nu}{d \langle TKE \rangle} [TKE - \overline{TKE}(A)] \right). \quad (1)$$

Based on the anti-correlation of neutron multiplicity associated with the complementary fission fragments observed by Vorobyev *et al.* [21] in the case of the reaction $^{252}\text{Cf}(\text{sf})$, a term obeying a Gaussian distribution with an average 0 and a standard deviation $\bar{\nu}_s(A)/3$ is added to $\nu_s(A, TKE)$ and a similar term with a standard deviation $\bar{\nu}_s(240 - A)/3$ is subtracted from $\nu_s(240 - A, TKE)$.

The conservation relations of mass, energy, and linear momentum of the primary fragments with masses A and A' , are the following:

$$A + A' = A_0, \quad (2)$$

where $A_0 = 240$, and

$$AE = A'E'. \quad (3)$$

3. Output data of the simulation

The output data are quantities assumed to be measured by the 2E technique associated with the complementary fragments, *i.e.*, the mass (μ and μ' , respectively) and the kinetic energy (e and e' , respectively). For the output data, as a function of the fragment mass calculated by the 2E method (μ), the following quantities are obtained: the yield (y . See Fig. 1); the distribution of the total kinetic energy of final complementary fragments ($tke = e + e'$) with its average (\overline{tke} . See Fig. 2) and its standard deviation (σ_{tke} . See Fig. 3); and the average prompt neutron multiplicity ($\bar{\nu}_\mu$. See Fig. 4). Due to the loss in mass by neutron evaporation, the values of the kinetic energy of final complementary fragments are, approximately,

$$e = E \left(1 - \frac{n}{A} \right), \quad (4a)$$

and

$$e' = E' \left(1 - \frac{n'}{A'} \right). \quad (4b)$$

With the double energy technique, e and e' are measured. To calculate the “pseudo” mass of complementary fragments (μ and μ' , respectively) the conservation relations 2 and 3 are applied to those quantities, *i.e.*,

$$\mu + \mu' = A_0, \quad (5)$$

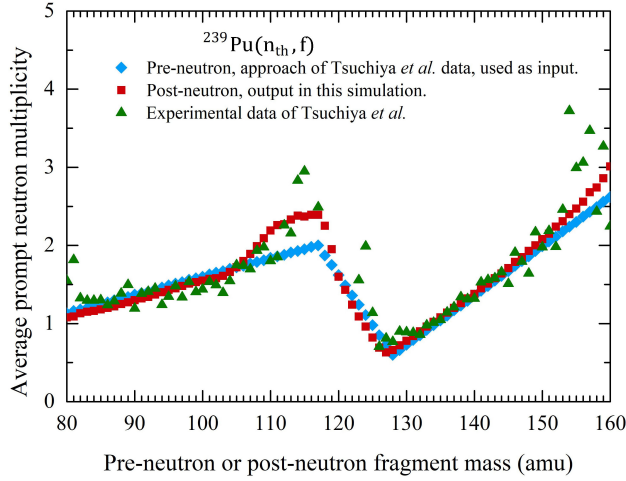


FIGURE 4. The average neutron multiplicity (measured by the 2E technique), as a function of the mass of fragments from the $^{239}\text{Pu}(\text{n}_{\text{th}}, \text{f})$ reaction. We show the simulated average prompt neutron multiplicity as a function of the primary fragment mass ($\bar{\nu}_s$, diamonds) and the corresponding to fragment pseudo mass output of simulation ($\bar{\nu}_\mu$, squares), compared with the corresponding to the experimental data taken from Ref. [13] ($\bar{\nu}$, triangles).

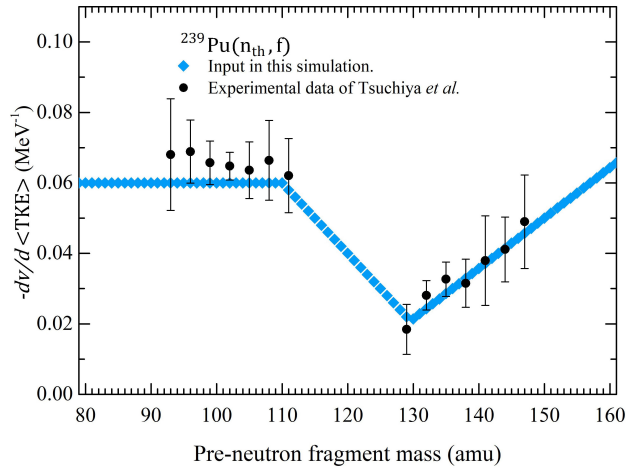


FIGURE 5. Simulation of the measurement by the 2E technique of the average neutron multiplicity as a function of the mass of fragments from $^{239}\text{Pu}(\text{n}_{\text{th}}, \text{f})$ reaction. The slope of neutron multiplicity against total kinetic energy, $-dv/d < TKE >$ (MeV^{-1}), plotted as a function of primary fragment mass (diamonds) an approach from the experimental data (circles) from Ref. [13].

and

$$\mu e = \mu' e'. \quad (6)$$

From Eqs. (4)-(6), we obtain

$$\mu = 240 \frac{E'}{TE + E'}, \quad (7)$$

where

$$T = \frac{1 - \frac{n}{A}}{1 - \frac{n'}{A}}. \quad (8)$$

4. Results

In the fragment mass region around $A \approx 115$, referred to the $Y(A)$ curve, the yield curve of the calculated mass $y(\mu)$ is shifted to higher mass values. See Fig. 1. This effect occurs because, in that region, in average, $n > n'$ (See Fig. 4) and $A \approx A'$, then $T < 1$. Consequently, from Eq. (7), we deduce that

$$\mu > A. \quad (9)$$

In the fragment mass region around $A \approx 125$, referred to the $Y(A)$ curve, the yield of the calculated mass $y(\mu)$ is shifted to lower mass values. See Fig. 1. This effect occurs because, in that region, in average, $n < n'$ (See Fig. 4) and $A \approx A'$, then $T > 1$. Consequently, from Eq. (7), we deduce that

$$\mu < A. \quad (10)$$

In general, the average final total kinetic energy ($\overline{\text{tke}}$) is lower than the average primary total kinetic energy ($\overline{\text{TKE}}$). See Fig. 2. This is explained by Eqs. (4a) and (4b).

Curve $\overline{\text{TKE}}$ shows a discontinuity in $A = 140$. In the same pseudo mass value, *i.e.*, $\mu = 140$, σ_{tke} is higher than the average between the neighboring values corresponding to $\mu=139, 141$. See Figs. 2 and 3, respectively. This result is because primary masses neighboring to 140, with different kinetic energy distributions, converge to $\mu = 140$. Similar behavior occurs in the mass region around $A = 122, 123$.

Figure 4, we represent the simulated average of prompt neutron multiplicity as a function of the pseudo mass $\bar{\nu}_\mu(\mu)$. In the mass regions around $A = 115$ and $A > 150$, where $\mu > A$ and Y_A is a decreasing function of fragment mass, an overestimation of $\bar{\nu}_\mu(\mu)$ referred to $\bar{\nu}_s$ is observed. Our results on $\bar{\nu}_\mu(\mu)$ reproduce the experimental data of Tsuchiya

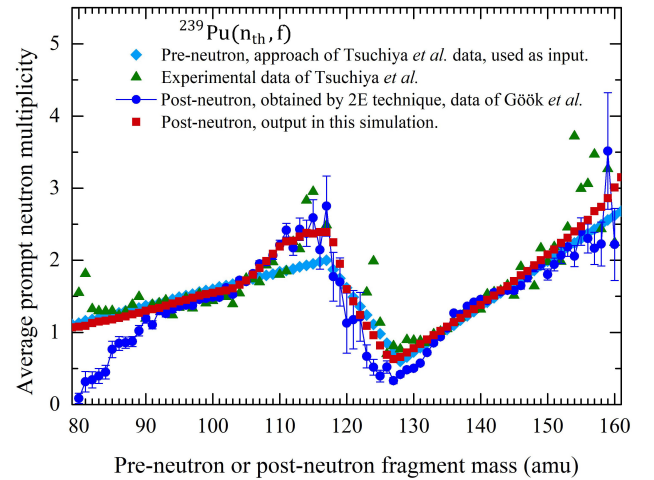


FIGURE 6. The average neutron multiplicity (measured by the 2E technique), as a function of the mass of fragments from the $^{239}\text{Pu}(\text{n}_{\text{th}}, \text{f})$ reaction. We show the simulated average prompt neutron multiplicity as a function of the primary fragment mass ($\bar{\nu}_s$, diamonds) and the corresponding to the fragment pseudo mass output of simulation ($\bar{\nu}_\mu$, squares), compared with the corresponding to the experimental data of Tsuchiya *et al.* [13] and with Gök *et al.* [18], respectively.

et al. [13] and Gök *et al.* [18], respectively. See Fig. 6. To interpret those results, we use the definition of the average prompt neutron multiplicity as a function of pseudo mass, *i.e.*,

$$\bar{\nu}_\mu(\mu) = \frac{n_{\max} Y_{A=\mu-n_{\max}} + (n_{\max} - 1) Y_{A=\mu-n_{\max}+1} + \dots + 1 Y_{A=\mu-1} + 0 Y_{A=\mu}}{Y_{A=\mu-n_{\max}} + Y_{A=\mu-n_{\max}+1} + \dots + Y_{A=\mu-1} + Y_{A=\mu}}, \quad (11)$$

where $Y_{A=\mu-n}$ is the yield of primary fragment mass $\mu - n$ that emitted n neutrons. From this equation, we can deduce that if the mass yield Y_A is constant as a function of primary mass A , then $\bar{\nu}_\mu = \bar{\nu}_A$; and, if it is a decreasing (increasing) function of A , then $\bar{\nu}_\mu > \bar{\nu}_A$ ($\bar{\nu}_\mu < \bar{\nu}_A$).

5. Discussion

We simulated the measurement, by the 2E technique, of the average prompt neutron multiplicity as a function of fragment

mass for the $^{239}\text{Pu}(\text{nth}, \text{f})$ reaction. Compared to input values $\bar{\nu}_s(A)$, an overestimation of the output values $\bar{\nu}_\mu(\mu)$ in the mass regions $A \approx 115$ and $A > 150$, respectively, is observed. This behavior is because, in those mass regions, there are two conditions: i) Y is a decreasing function of A and ii) $\mu > A$. The result of the simulation suggests that, in those mass regions, the 2E experimental values ($\bar{\nu}_e$), referred to the primary quantities ($\bar{\nu}$), are overestimated.

1. S. Bjørnholm and J. E. Lynn, The double-humped fission barrier, *Rev. Mod. Phys.* **52** (1980) 725, <https://doi.org/10.1103/RevModPhys.52.725>.
2. E. E. Maslin, A. L. Rodgers, and W. G. F. Core, Prompt neutron emission from U235 fission fragments, *Phys. Rev.* **164** (1967) 1520, <https://doi.org/10.1103/PhysRev.164.1520>.
3. K. Nishio, Y. Nakagome, H. Yamamoto, and I. Kimura, Multiplicity and energy of neutrons from $^{235}\text{U}(\text{nth}, \text{f})$ fission fragments, *Nucl. Phys. A.* **632** (1998) 540, [https://doi.org/10.1016/S0375-9474\(98\)00008-6](https://doi.org/10.1016/S0375-9474(98)00008-6).
4. A. S. Vorobyev, O. A. Shcherbakov, A. M. Gagarski, G. V. Val'ski, and G. A. Petrov, Investigation of the prompt neutron emission mechanism in low energy fission of $^{235,233}\text{U}(\text{nth}, \text{f})$ and $^{252}\text{Cf}(\text{sf})$, *EPJ Web Conf.* **8** (2010) 03004, <https://doi.org/10.1051/epjconf/20100803004>.
5. A. Gök, F.-J. Hamsch, S. Oberstedt, and M. Vidali, Prompt neutrons in correlation with fission fragments from U235 (n,f), *Phys. Rev. C.* **98** (2018) 044615, <https://doi.org/10.1103/PhysRevC.98.044615>.
6. C. Signarbieux, J. Poitou, M. Ribrag, and J. Matuszek, Correlation entre les energies d'excitation des deux fragments complementaires dans LA fission spontanee de ^{252}Cf , *Phys. Lett. B.* **39** (1972) 503, [https://doi.org/10.1016/0370-2693\(72\)90330-9](https://doi.org/10.1016/0370-2693(72)90330-9).
7. R. L. Walsh and J. W. Boldeman, Fine structure in the neutron emission $\nu(A)$ from ^{252}Cf spontaneous fission fragments, *Nucl. Phys. A.* **276** (1977) 189, [https://doi.org/10.1016/0375-9474\(77\)90378-5](https://doi.org/10.1016/0375-9474(77)90378-5).
8. V. P. Zakharova and D. Ryazanov, Neutron yields from spontaneous fission of ^{252}Cf , *Sov. J. Nucl. Phys.* **30** (1979) 19, [*Sov. J. Nucl. Phys.* **30** (1979) 19].
9. C. Budtz-Jørgensen and H.-H. Knitter, Simultaneous investigation of fission fragments and neutrons in $^{252}\text{Cf}(\text{SF})$, *Nucl. Phys. A.* **490** (1988) 307, [https://doi.org/10.1016/0375-9474\(88\)90508-8](https://doi.org/10.1016/0375-9474(88)90508-8).
10. V. N. Dushin *et al.*, Facility for neutron multiplicity measurements in fission, *Nucl. Instruments Methods Phys. Res. Sect. A Accel. Spectrometers, Detect. Assoc. Equip.* **516** (2004) 539, <https://doi.org/10.1016/j.nima.2003.09.029>.
11. V. F. Apalin, Y. N. Gritsyuk, I. E. Kutikov, V. I. Lebedev, and L. A. Mikaelian, Neutron emission from U233, U235 and Pu239 fission fragments, *Nucl. Phys.* **71** (1965) 553, [https://doi.org/10.1016/0029-5582\(65\)90765-0](https://doi.org/10.1016/0029-5582(65)90765-0).
12. K. Nishio, Y. Nakagome, I. Kanno, and I. Kimura, Measurement of Fragment Mass Dependent Kinetic Energy and Neutron Multiplicity for Thermal Neutron Induced Fission of Plutonium-239, *J. Nucl. Sci. Technol.* **32** (1995) 404, <https://doi.org/10.1080/18811248.1995.9731725>.
13. C. Tsuchiya *et al.*, Simultaneous measurement of prompt neutrons and fission fragments for $^{239}\text{Pu}(n_{\text{th}}, \text{f})$, *J. Nucl. Sci. Technol.* **37** (2000) 941, <https://doi.org/10.1080/18811248.2000.9714976>.
14. O. A. Batenkov *et al.*, Prompt neutron emission in the neutron-induced fission of ^{239}Pu and ^{235}U , *AIP Conference Proceedings.* **769** (2005) 1003, <https://doi.org/10.1063/1.1945175>.
15. M. Montoya, Behavior of the average prompt neutron multiplicity as a function of post-neutron fragment mass in correlation with the pre-neutron fragment mass distribution in thermal neutron induced fission of ^{235}U and ^{233}U , *Results Phys.* **14** (2019) 102356, <https://doi.org/10.1016/j.rinp.2019.102356>.
16. M. Montoya and C. Romero, Correlation between the average prompt neutron multiplicity as a function of the primary mass and the corresponding experimental mass of fragments from ^{252}Cf spontaneous fission, *Results Phys.* **15** (2019) 102685, <https://doi.org/10.1016/j.rinp.2019.102685>.

17. M. Montoya, Oversize of the average prompt neutron multiplicity measured by the IVIE method in the symmetric region of thermal neutron-induced fission of ^{239}Pu , *Results Phys.* **17** (2020) 103053, <https://doi.org/10.1016/j.rinp.2020.103053>.
18. A. Göök, F.-J. Hamsch, and S. Oberstedt, Neutron Multiplicity Correlations with Fission Fragment Mass and Energy from $^{239}\text{Pu}(n, f)$, *EPJ Web Conf.* **239** (2020) 05009, <https://doi.org/10.1051/epjconf/202023905009>.
19. R. Vogt, J. Randrup, D. A. Brown, M. A. Descalle, and W. E. Ormand, Event-by-event evaluation of the prompt fission neutron spectrum from $^{239}\text{Pu}(n, f)$, *Phys. Rev. C.* **85** (2012) 024608, <https://doi.org/10.1103/PhysRevC.85.024608>.
20. M. Asghar, F. Caiucoli, P. Perrin, and C. Wagemans, Fission fragment energy correlation measurements for the thermal neutron fission of ^{239}Pu and ^{235}U , *Nucl. Physics, Sect. A.* **311** (1978) 205, [https://doi.org/10.1016/0375-9474\(78\)90510-9](https://doi.org/10.1016/0375-9474(78)90510-9).
21. A. S. Vorobyev, Distribution of Prompt Neutron Emission Probability for Fission Fragments in Spontaneous Fission of ^{252}Cf and $^{244,248}\text{Cm}$, *AIP Conference Proceedings.* **769** (2005) 613, <https://doi.org/10.1063/1.1945084>.